

Long-Range Time Correlations in Plasma Edge Turbulence

B. A. Carreras,¹ B. van Milligen,² M. A. Pedrosa,² R. Balbín,² C. Hidalgo,² D. E. Newman,¹ E. Sánchez,² M. Frances,²
I. García-Cortés,² J. Bleuel,³ M. Endler,³ S. Davies,⁴ and G. F. Matthews⁴

¹*Oak Ridge National Laboratory, Oak Ridge, Tennessee 37831-8070*

²*Asociación Euratom-Ciemat, 28040 Madrid, Spain*

³*Max-Planck-Institut für Plasmaphysik, Euratom Association, 85740 Garching, Germany*

⁴*JET Joint Undertaking, Abingdon, Oxon, OX14 3EA, United Kingdom*

(Received 20 January 1998)

Analysis of the edge plasma fluctuation in several confinement devices reveals the self-similar character of the fluctuations through the presence of long-range time correlations. These results show that the tail of the autocorrelation function decays as a power law for time lags longer than the decorrelation time and as long as times on the order of the particle diffusion time. The algebraic decay of the long-range time correlations is consistent with plasma transport characterized by self-organized criticality. [S0031-9007(98)06077-3]

PACS numbers: 52.55.Fa, 52.25.Gj, 52.35.Ra, 52.55.Hc

Complex natural systems are often governed by self-organized criticality (SOC). The concept of SOC [1] brings together the ideas of self-organization of nonlinear dynamical systems with the often observed near-critical behavior of many natural phenomena. These phenomena exhibit self-similarities over extended ranges of spatial and temporal scales. In such systems, scale lengths may be described by fractal geometry and time scales that lead to a power spectra that decreases as the inverse of the frequency ($1/f$ -like). Self-organized criticality provides an intimate connection between scale invariance in both space and time.

It has been suggested that the SOC approach should be used to understand some characteristics of plasma transport [2,3]. Numerical plasma turbulence calculations [4] including profile evolution have shown some of the characteristic properties of the SOC systems: existence of a critical profile gradient and transport by avalanches. There is some indirect experimental evidence for SOC behavior of magnetically confined plasmas in the so-called low confinement regime. Phenomena such as the resilience of plasma profiles to changes in the location of the heating source and Bohm scaling of the diffusivities could be consequences of SOC dynamics. Self-organized criticality may also explain some of the nonlocal behavior often observed in perturbative experiments. However, it is difficult to devise a direct test of transport by avalanches. The most obvious test would be the determination of propagating long-range radial correlations of the turbulence. Such a test is difficult to implement experimentally because it would require the simultaneous detection of fluctuations at many radial locations. Therefore, before planning such a complex experiment, it is convenient to look for long-range time correlations that can also be induced by avalanchelike transport.

In the present study, we consider low-power ohmically heated or electron cyclotron-heated (ECH) plasma dis-

charges. The SOC behavior of the bulk plasma transport is expected to be a characteristic of higher-power plasma discharges in the so-called low confinement regime. The reason for analyzing lower-power plasmas is that we study edge plasma fluctuations, and it is at the edge where the SOC behavior is expected to manifest itself first. As the power increases, this zone would extend toward the core and cause the characteristic confinement deterioration of the low confinement mode. Furthermore, at high power, the plasma edge will be in a continuous avalanching regime in which correlations are more difficult to detect because of the randomization caused by frequent overlapping.

We emphasize that our goal is the identification of long-time dependencies in the fluctuation data. In other words, we study how the tail of the autocorrelation function of the fluctuations decays. The autocorrelation function of the edge plasma fluctuations has a narrow peak at time lag zero and a slowly decaying tail (that may have oscillations). The peak of the autocorrelation function carries information on the correlation of the local fluctuations, while the information on avalanches would be revealed by an algebraic decay of the long-time correlated events. Such an algebraic decay of the probability distribution function of the avalanche durations is a characteristic of a SOC system [5,6].

To accurately determine the tail of the probability distribution function, very good statistics are required. This is a problem for plasma turbulence studies in magnetically confined devices because of the short duration of the plasma discharges. However, there are techniques that seem to be effective for the determination of long-range dependencies in a finite time series. One such method is the rescaled adjusted range statistics (R/S statistics) proposed by Mandelbrot and Wallis [7] and based on a previous hydrological analysis by Hurst [8].

For a time series of length n , $X \equiv \{X_t: t = 1, 2, \dots, n\}$, with mean $\bar{X}(n)$ and variance $S^2(n)$, the R/S ratio is defined as

$$\frac{R(n)}{S(n)} = \frac{\max(0, W_1, W_2, \dots, W_n) - \min(0, W_1, W_2, \dots, W_n)}{\sqrt{S^2(n)}}, \quad (1)$$

where $W_k = X_1 + X_2 + \dots + X_k - k\bar{X}(n)$. For a sequence with short-range dependencies, of which a random signal is an extreme case, the expected value of this ratio scales as $E[R(n)/S(n)] \xrightarrow{n \rightarrow \infty} \lambda n^{0.5}$. However, for phenomena characterized by long-range dependencies, it scales as $E[R(n)/S(n)] \xrightarrow{n \rightarrow \infty} \lambda n^H$, with $H > 0.5$. Here, H is the so-called Hurst parameter. A constant H parameter over a long range of time lag values is consistent [9] with self-similarity of the signal and an autocorrelation function $\rho_h^{(m)} = \delta^2(h^{2-\beta})/2$. Here, the superscript m indicates the autocorrelation for the averaged process $X^{(m)} \equiv \{X_u^{(m)}: u = 1, 2, \dots, n/m\}$ resulting from averaging the original sequence over nonoverlapping blocks of size m , $X_u^{(m)} = (X_{um-m+1} + \dots + X_{um})/m$. The operator δ^2 is the second-order central derivative operator in finite differences, h is the time lag, and $\beta = 2 - 2H$. In comparison with the direct determination of the autocorrelation function or other alternative techniques of calculating the value of H , the R/S analysis is robust [10].

In the present study, the data analyzed are edge Langmuir probe measurements from three stellarators, TJ-IU [$\bar{n}_e = (1-5) \times 10^{18} \text{ m}^{-3}$, $B_T = 0.67 \text{ T}$] [11], W7-AS [$\bar{n}_e = (1-2) \times 10^{19} \text{ m}^{-3}$, $B_T = (1.25-2.52) \text{ T}$] [12], and ATF [$\bar{n}_e = (3-6) \times 10^{18} \text{ m}^{-3}$, $B_T = 1 \text{ T}$] [13], in the ECH heat regime. We have also considered two tokamaks, TJ-I [$\bar{n}_e = (1-2) \times 10^{19} \text{ m}^{-3}$, $B_T = (0.8-1.4) \text{ T}$], and JET [$\bar{n}_e = (1-2) \times 10^{19} \text{ m}^{-3}$, $B_T = 2.6 \text{ T}$] [15], in the Ohmic heated regime. Here, \bar{n}_e is the averaged plasma density and B_T is the toroidal magnetic field. The available data correspond to radial probe scans with positions that are close and within the edge sheared flow layer. A summary of the results of the analysis is given in Table I.

A typical plot of R/S versus time lag is shown in Fig. 1. For time lags smaller than a few decorrelation times, there is a transient with a nearly constant slope, with a value close to 0.9 in general. After this initial phase, R/S settles on an ‘‘asymptotic’’ power law (continuous line in Fig. 1) that is used to determine the value of H . The last few points on the high-lag end are not taken into consideration because they lack statistical significance, because the size of the subblocks is of the order of the size of the time sample. The error bars are estimated by the statistical dispersion of the results from the different subblocks of data. The range of the time lags over which H is determined is the ‘‘self-similarity range’’ given in Table I for each data set. Typically, they are several orders of magnitude longer than the turbulence decorrelation time, and in most cases the upper limit is set by the availability of data. The turbulence decorrelation time τ_D is the autocorrelation time estimated at the zero velocity point in the shear layer for each data set.

The main result of our analysis is that, for all data sets, the Hurst parameter is constant and well above 0.5 over the self-similarity range. This result is a clear indication of the existence of long-range dependencies in the fluctuation dynamics. Because the self-similarity range involves time lags from the fluctuation time scales to transport time scales, it is also an indication that there is no clear separation of time scales between the fluctuation and the transport dynamics. In Table I, $\langle H \rangle_{\text{in}}$ is the radial average of H in the plasma edge and $\langle H \rangle_{\text{out}}$ in the scrape-off layer. The \pm indicates the radial variation of H ; it is not an error bar. Within the plasma, the Hurst parameter varies between 0.62 and 0.75, a relatively small range given the diversity of plasma confinement devices considered. In the scrape-off layer, the values of H have a broader range of variation. This variation could reflect the diversity of scrape-off-layer conditions for the devices considered and also the loss of scrape-off-layer behavior outside the last closed flux surface. In Fig. 2, we have plotted the radial profile of H for three stellarator configurations. We use as the ‘‘radial’’ variable x the distance in real space between the position of the probe and the zero-velocity point in the shear flow layer, and we do not take into account the geometry of the

TABLE I. Summary of the data analyzed. In the table, $\langle H \rangle_{\text{in}}$ ($\langle H \rangle_{\text{out}}$) is the averaged value of the Hurst exponent in the plasma edge, $x > 0$ (scrape-off layer, $x < 0$), region of the plasma (see Fig. 2). In the case of W7-AS, two configurations with different edge rotational transforms ι_a are considered.

Device	Number of time series	$\langle H \rangle_{\text{in}}$	$\langle H \rangle_{\text{out}}$	τ_D (μs)	Self-similarity range (ms)
TJ-1	9	0.75 ± 0.03	0.75 ± 0.04	3.0	0.1–2.0
JET limiter	4	...	0.52 ± 0.04	29.0	0.1–2.0
JET divertor	4	...	0.63 ± 0.03	19.0	0.1–2.0
TJ-IU stellarator	21	0.64 ± 0.03	0.67 ± 0.01	6.0	0.1–2.0
W7-AS $\iota_a = 0.243$	24	0.62 ± 0.01	0.60 ± 0.04	20.0	1–20
W7-AS $\iota_a = 0.355$	29	0.72 ± 0.07	0.66 ± 0.06	19.0	1–20
ATF	20	0.71 ± 0.03	0.92 ± 0.07	34.0	1–12

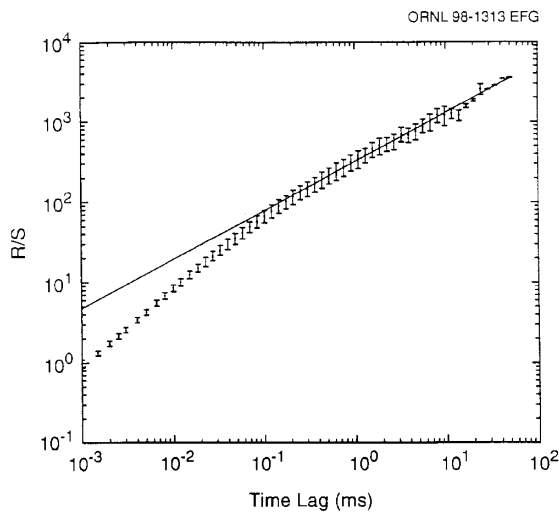


FIG. 1. Plot of the expected value of R/S as a function of the time lag for one of the time series of W7-AS with $\nu_a = 0.243$. The continuous line is a power fit to the asymptotic values.

flux surfaces. Negative values of x correspond to the scrape-off layer and positive ones to the edge plasma region. This figure illustrates the different behavior in the scrape-off layer. A similar conclusion may be drawn from the two JET results in Table I that corresponds to the same discharge parameters operating initially in a limiter configuration and switching later to a divertor configuration. Unlike the other devices, the JET data sets are much shorter than the confinement time of the device.

Potential problems in the determination of H are the existence of coherent MHD instabilities or sawtooth oscillations and plasma drifts. These phenomena produce a clear signal in the value of R/S that, although they cannot be confused with long-range dependencies in the

turbulence, do not allow the extraction of the value of H . A careful selection of the data is needed to avoid samples dominated by plasma drifts. However, these phenomena do not produce misleading interpretations for H because they carry clear signatures that allow the exclusion of data that do not provide information on the plasma turbulence. The consistent determination of H has also been cross-checked with the determination of the scaling with the lag of the variance and probability of return. These details of the analysis will be discussed elsewhere. In the case of stellarators, magnetic islands may be present in the scrape-off layer ($\nu_a \sim 1$ in ATF and $\nu_a \sim 0.25$ in W7-AS). The effect of such magnetic islands on the fluctuation, and therefore H , is not yet clear.

The calculation of H is rather robust. In Fig. 3, we have plotted the radial profile of H for three plasma discharges in W7-AS with similar plasma parameters and corresponding to a configuration with edge rotational transform $\nu_a = 0.243$. The error bars are calculated from a power fit to R/S taking into account the statistical error in the individual estimates of R/S . Although the error bars are comparable to the radial variation, the radial profile is reproducible. In Fig. 2, we have plotted the radial profiles that result from averaging over these three discharges. The situation is similar for the other configurations,

Cellular automata based on the sandpile dynamics have been a standard model in studying generic properties of self-organized criticality [1,6]. The model is based on the existence of a critical sandpile slope. When by random addition of grains of sand the critical slope is reached, grains of sand fall down the pile in a prescribed manner. The dynamical process shows that in steady state the sandpile slope is, in averaged sense, well below the critical slope and yet the transport of sand is still produced

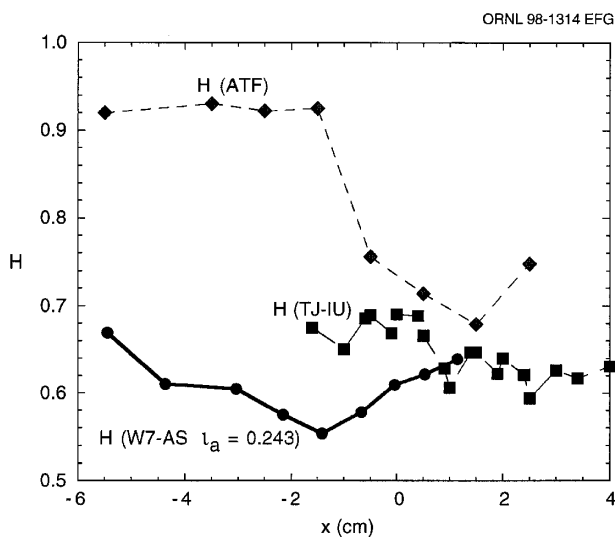


FIG. 2. Radial profile of the Hurst parameter H for three different edge magnetic configurations. The shear layer location has been used as a point of reference.

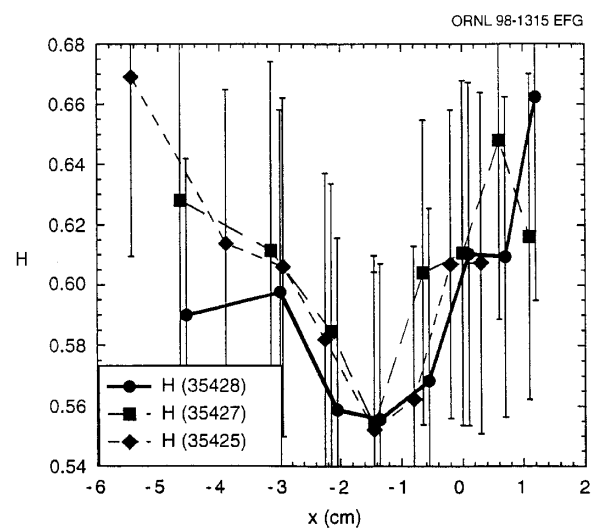


FIG. 3. Radial profile of the Hurst parameter H for three different plasma discharges with the same global parameters in W7-AS and for the configuration with $\nu_a = 0.243$.

by avalanches. These avalanches have length scales that vary from a single cell up to the full size of the system. In the dynamical evolution of the sandpile, all of the cells are checked for stability against a simple stability rule and either flagged as stable or not before the cells are time advanced. After that, the cells are time evolved with the unstable cells overturning and moving their excess grains to another cell. The size, distance, and direction of the motion of the excess grains are determined by the overturning rule.

The R/S analysis of sandpile data (number of cells overturning in each time step) in a regime of weak avalanche overlap gives a constant value of H over many decades. This value is around 0.8, with a slight variation from case to case depending on the probability of adding grains to the sandpile. As shown by previous calculations, the addition of a sheared flow to the sandpile induces a decorrelation of avalanches [16]. This decorrelation effect is also shown by the change in the value of H . When a sheared flow is added to the sandpile, the long-range correlations are eliminated, and H is close to 0.5.

There is some indication in the analyzed data that the sheared flow effect could also be present at the plasma edge turbulence. In Fig. 2, there is a change in the radial dependence of H near the shear flow layer. This effect is weak, and it is not possible to distinguish from a change caused by crossing to the scrape-off layer. Not all of the profile changes are aligned with the zero of the shear flow; however, we have not measured the plasma flow directly. Here, the shear flow layer is defined from the measurement of the phase velocity of the fluctuations and the flow profiles are different for the different configurations. Therefore, the maximum shear in the $\mathbf{E} \times \mathbf{B}$ flow may be somewhat displaced from the zero-velocity position.

The effect of reducing H by shear flow is different from the reduction of the decorrelation time of the turbulence first determined in the TEXT tokamak [17] and later seen in other devices [18]. The dynamics governing the decorrelation of the local fluctuations and the long-range time dependencies are probably different, one being the decorrelation of the turbulence and the other being the decorrelation of the transport events (avalanches) [4].

Finally, it is important to realize that the fluctuation measurements used in the present analysis correspond to plasmas with a differential rotation in the poloidal direction with respect to the laboratory frame. Thus, the long-range dependencies identified here must not necessarily be long range in time; they could be the reflection of long-range dependencies in the poloidal variable. In either case, the presence of such dependencies is consistent with plasma transport mechanisms based on avalanches.

In conclusion, analysis of the edge plasma fluctuations in several confinement devices indicates that the fluctua-

tions are characterized by self-similarity and long-range time correlations. Therefore, the tail of the turbulence autocorrelation function decays as a power law for time lags longer than the decorrelation time and as long as times of the order of the energy and particle confinement times (characteristic time for particle and energy to diffuse across the edge region). Calculations show that long-range time correlations are reduced or even eliminated by shear flow effects. In the experiments, the sheared flows are not strong enough to suppress turbulence, but there are indications that the long-range time correlations are modified by a shear flow. These results are consistent with self-organized criticality behavior and plasma transport mechanisms based on avalanches. More systematic analysis of data from other confinement devices is needed to confirm these conclusions. In particular, measurements comparing long-range radial correlations should be compared with long-range time correlations.

Oak Ridge National Laboratory is managed by Lockheed Martin Energy Research Corp. for the U.S. Department of Energy under Contract No. DE-AC05-96OR22464.

-
- [1] P. Bak, C. Tang, and K. Wiesenfeld, *Phys. Rev. Lett.* **59**, 381–384 (1987).
 - [2] P. H. Diamond and T. S. Hahm, *Phys. Plasmas* **2**, 3640–3649 (1995).
 - [3] D. E. Newman *et al.*, *Phys. Plasmas* **3**, 1858–1866 (1996).
 - [4] B. A. Carreras *et al.*, *Phys. Plasmas* **3**, 2903–2911 (1996).
 - [5] L. P. Kadanoff *et al.*, *Phys. Rev. A* **39**, 6524–6537 (1989).
 - [6] T. Hwa and M. Kadar, *Phys. Rev. A* **45**, 7002–7023 (1992).
 - [7] B. B. Mandelbrot and J. R. Wallis, *Water Resour. Res.* **4**, 909–918 (1969).
 - [8] H. E. Hurst, *Trans. Am. Soc. Civil Eng.* **116**, 770 (1951).
 - [9] G. Samorodnitsky and M. S. Taqqu, *Stable Non-Gaussian Random Processes: Stochastic Models with Infinite Variance* (Chapman and Hall, New York, 1994).
 - [10] B. B. Mandelbrot and J. R. Wallis, *Water Resour. Res.* **5**, 967–988 (1969).
 - [11] C. Hidalgo *et al.*, *Phys. Rev. Lett.* (to be published).
 - [12] J. Bleuel *et al.*, in *Controlled Fusion and Plasma Physics* (European Physical Society, Kiev, 1996), Vol. 20C, pp. 727–730.
 - [13] C. Hidalgo *et al.*, *Nucl. Fusion* **13**, 1471–1478 (1991).
 - [14] I. Garcia-Cortes *et al.*, *Phys. Fluids B* **4**, 4007–4011 (1992).
 - [15] I. Garcia-Cortes *et al.*, in *Controlled Fusion and Plasma Physics* (European Physical Society, Berchtesgarden, 1997), Vol. 21A, Pt. 1, pp. 109–112.
 - [16] D. E. Newman, B. A. Carreras, and P. H. Diamond, *Phys. Lett. A* **218**, 58–63 (1996).
 - [17] C. P. Ritz *et al.*, *Phys. Rev. Lett.* **65**, 2543–2546 (1990).
 - [18] K. H. Burrell, *Phys. Plasmas* **4**, 1499–1518 (1997).